Phenology Modelling and Forest Disturbance Mapping with Sentinel-2 time series in Austria

Markus Löw (markusloew@gmx.at)
Universitat fur Bodenkultur Wien https://orcid.org/0000-0002-6622-6497
Koukal Tatjana
Austrian Research Center for Forests, Department of Forest Inventory

Research

Keywords: phenology modelling, forest disturbance, forest monitoring, bark beetle infestation, forest management, time series analysis, remote sensing, satellite imagery, Sentinel-2

Posted Date: May 6th, 2020

DOI: https://doi.org/10.21203/rs.3.rs-26379/v1

Abstract

Background Worldwide, forests provide natural resources and ecosystem services. However, forest ecosystems are threatened by increasing forest disturbance dynamics, caused by direct human activities or an altering natural environment. It is decisive to trace the intra- to trans-annual dynamics of these forest ecosystems. National to local forest communities request detailed area-wide maps that delineate forest disturbance dynamics at various spatial scales.

Methods We developed a remote sensing based time series analysis (TSA) framework that comprises data access, data management, image pre-processing, and an advanced but flexible TSA. The data basis is a dense time series of multispectral Sentinel-2 images with a spatial resolution of 10 metres. We use a dynamic Savitzky-Golay-filtering approach to reconstruct robust but sensitive phenology courses. Deviations from the latter are further used to derive spatiotemporal information on forest disturbances. In a first case study, we apply the TSA to map forest disturbances directly or indirectly linked to recurring bark beetle infestation in Northern Austria. Finally, we use zonal statistics on different spatial scales to provide aggregated information on the extent of forest disturbances between 2018 and 2019.

Results and Conclusion The outcomes are a) individual phenology models and deduced phenology metrics for each 10 metres by 10 metres forest pixel in Austria and b) forest disturbance maps useful to investigate the occurrence, development and extent of bark beetle infestation. The phenology modelling results provide area-wide consistent data, also useful for downstream analyses (e.g. forest type classification). Results of the forest disturbance detection demonstrate that the TSA is capable to systematically delineate disturbed forest areas. Information derived from such a forest monitoring tool is highly relevant for various stakeholders in the forestry sector, either for forest management purposes or for decision-making processes on different levels.

Background

Worldwide forests are increasingly affected by changes and dynamics of various origin and at different scales (Kindermann et al. 2008; Hansen et al. 2013; Mackey et al. 2015). Shifting patterns in timber use demands (FAO; Henders et al. 2015) or in silvicultural perceptions (O'Hara 2016) can constitute "sustainable" forest management, but can also trigger a change in timber harvest practises, including illegal logging and vast deforestation processes. Further, climate change effects on forest ecosystems accelerate forest mortality worldwide (McDowell et al. 2015). Forest biomes are the main terrestrial carbon stock (Birdsey and Pan 2015). Without doubt there is an urgent need to safeguard forested areas worldwide and trace dynamics of altering site conditions caused by climate change (Goetz and Dubayah 2011; McDowell et al. 2015). At the same time, forest product supply must be ensured, despite an increased multi-use demand concerning forest ecosystem functions (Matthews et al. 2000). Therefore, the future monitoring of vague and minimal land cover changes such as those caused by natural events (e.g. pest infestation, higher mortality due to altering site conditions) or forest management practices (e.g. thinning or selective timber extraction) becomes more and more crucial (Birdsey and Pan 2015).

Recent studies underlined the importance of a vital forest at stand or even single-tree level (Bastin et al. 2019). Forest disturbances can decrease the capability of forest ecosystems to protect against natural hazards, which is a major regulating function, especially of mountainous forests (Sebald et al. 2019). From a global perspective, it will not be sufficient to avoid deforestation to meet global climate change mitigation goals. Small-scale forest management has to be guided by the principles of sustainability too, because forest management has an unexpectedly large impact on standing biomass and related carbon sequestration (Erb et al. 2018). On the one hand, sustainable extraction of various forest products guarantees a young age structure, which can increase carbon sequestration rates up to 25% (Pugh et al. 2019). On the other hand, in mountainous terrain unmanaged forests show a higher capacity of climate and erosion self-regulation compared to managed forests. Therefore, natural forests are more resilient to altering environmental conditions and will provide valuable regulating ecosystem services in the future (Seidl et al. 2019). The monitoring of such small-scale forest management practices will be crucial to guarantee a sustainable forestry, not only in Austria.

Earth observation data proved to be a comprehensive source to continuously assess the state of forests and to detect disturbances globally. Today image processing and analysis tools can map these changes and are increasingly capable to trace slight phenology anomalies on different temporal scales, informing about intra-, inter- and trans-annual dynamics (Goetz and Dubayah 2011; McDowell et al. 2015).

During the last decades, EO-programmes as LANDSAT (Wulder et al. 2019) or MODIS (García-Mora et al. 2012) deliver data, which have enabled the implementation of large scale monitoring systems (e.g. Global Forest Watch, based on data of (Hansen et al. 2013)), as data provision is continuous and data quality consistent.

However, a phenological time series analysis (TSA) of global satellite imagery must cope with a highly varying topography and seasonal vegetation effects, compared to studies explicitly focusing on selected world regions that are less challenging (e.g. tropical forest or other biomes closer to the equator).

Austria, as an example of a country with diverse landscapes, shows distinct seasonality with low to high sun levels. The illumination conditions strongly vary, especially in alpine regions (topographic shadow areas), which affects the remotely sensed signal reflected by the Earth surface. During winter, snow cover and diverse weather patterns, such invasive fog that is omnipresent in alpine valleys, reduce the number of useful observations significantly.

Previous research shows different methodical approaches to cope with these challenges. Most of the mainly LANDSAT-based TSAs are based on an image composite analysis (Nguyen et al. 2018; Sebald et al. 2019) or on some variant of a harmonic modelling approach (Zhu and Woodcock 2014; Moisen et al. 2016; Pasquarella et al. 2017; Nguyen et al. 2018; Hermosilla et al. 2019; Sebald et al. 2019; Bullock et al. 2020). Harmonic modelling approach robust but shows some limitations regarding the quality of temporal information (Jönsson et al. 2018) and allow only little detail in reconstructing seasonal vegetation courses. This limits the ability to depict the development and magnitude of changes, which is needed to scrutinise dynamics on a forest management level. The new COPERNICUS programme, the

European Union's earth observation programme (European Space Agency 2020a), with its satellite twin consisting of Sentinel-2a and Sentinel-2b (S2) (European Space Agency 2020b) new opportunities for monitoring forest ecosystems. The multispectral S2 sensor shows a spatial, spectral, and temporal resolution so far unique in non-commercial EO. The ground resolution is up to 10m and the revisit time is less than five days. The use of S2 data that is free of charge is quite established in agricultural monitoring (Belgiu and Csillik 2018; Kanjir et al. 2018) and non-forest phenology modelling (Vrieling et al. 2018), whereas advanced S2-based TSAs focusing on forest ecosystems are so far rare.

The Austrian Research Centre for Forests (in German: Bundesforschungszentrum für Wald - BFW) is, as a central federal research institution, focusing on forest state and forest future (BFW 2020). The BFW's Department of Forest Inventory, responsible for the national forest inventory (NFI) in Austria, gathers, prepares and analyses nationwide information about forest state and dynamics (Gabler and Schadauer 2006). New earth observation data, such as the S2 imagery, are a good supplement for existing terrestrial inventory data. Area-wide auxiliary data from remote sensing encounters weaknesses of sample-based inventory assessments (Puliti et al. 2020; Breidenbach et al. 2020). The compilation of facts and figures for stakeholders and decision makers is a main task of the Austrian NFI. National to local forest communities increasingly request information concerning hot topics as storm damages, altering forest site conditions (e.g. tree species specific drought stress) or spatial patterns of pest invasions (e.g. the spread of bark beetle infestations). For these reasons, the BFW decided to establish a local archive for nationwide S2 data and to set up operational data processing schemes to optimally exploit the existing data pool. Within this framework, an operational forest monitoring approach based on S2 data has been developed.

This article describes the novel TSA approach, focusing on forest disturbances directly or indirectly linked to bark beetle infestation and in this regard to get the best out of the entire multi-spectral Sentinel-2 dataset, following five basic aims: (1) to reconstruct continuous, filtered, line-fitted and smoothed time series of different spectral vegetation indices (phenology courses), (2) to deduce comprehensive phenology features (phenology metrics) by multi-annual time series fusion, (3) to detect minor to major magnitude deviations from the modelled phenology courses, (4) to derive novel sensitive information about temporal characteristics of that changes (ranging from gradual to abrupt), (5) to provide forest disturbance maps both at pixel level and multiple aggregation levels.

Methods

Data preprocessing

The proposed TSA approach relies on multispectral Sentinel-2A & -2B data, provided freely via the COPERNICUS programme of the European Space Agency (ESA) (European Space Agency 2020a). The approach uses the Top-Of-Atmosphere product (TOA, Level-1C).

For covering the whole of Austria, 20 Seninel-2 granules are required. On a regular basis, missing observations of all granules are searched and operationally downloaded with an oData-query via the ESA API-hub (European Space Agency 2020c). The incoming imagery is saved on a local NAS-storage. Our imagery archive starts in 2017, when the ESA has set its final granule naming scheme.

Images with less than 80% cloud cover (L1C-meta-data-file) are pre-processed. The ESA's stand-alone atmospheric correction algorithm Sen2Cor (European Space Agency 2020d) is used to convert Level-1C (TOA) to Level-2A surface reflectance data (Bottom-of-Atmosphere, BOA). Topographic correction was deactivated, as Sen2Cor was found to be prone to overcorrection effects. Next, auxiliary grids (called MASKs) are generated to exclude pixels that are affected by clouds and shadows and areas that are not relevant for subsequent analyses, such as areas covered by water. The process relies on several L2A outputs (SCLL2A, CLDL2A, B08L2A) as well as shadow and overexposure proxies based on the near-infrared band and results in unique MASKs for each observation. The MASKs are stored on our NAS-storage.

Optionally, the data can be clipped to an area of interest and pixels that are not relevant can be excluded with the help of auxiliary grids (e.g. maps of vegetation height or tree cover type). In this study, we use a forest area layer, produced at the BFW according to the Austrian NFI forest definition, to dismiss non-forested areas. Now the data is ready to create multi-temporal layer stacks (three-dimensional arrays) using the four Sentinel-2 bands with a spatial resolution of 10 m (B01: blue, B02: green, B03: red and B08: near infrared). In theory, Bottom-of-Atmosphere (BOA) data are expected to be more suitable for time series analysis. However, it was found that BOA data produced by Sen2Cor are too error prone for a fully operational approach without any visual scene checking and selection. Besides, data reliability and continuity are decisive for detailed phenology modelling and a versatile forest disturbance mapping. Therefore, we use Level-1C data (TOA) to compile the raw time series. As signal noise between observations might be higher in TOA data compared to BOA data, we integrated an outlier detection and filtering techniques to minimise such noise effects.

Additionally, we use normalised spectral indices instead of single bands to further compensate for noise effects, as normalised indices are less affected by atmospheric and topographic effects than single band values (e.g. Xue and Su 2017). There is a huge number of spectral indices in literature suggested for vegetation analyses. In this study, we selected four indices; NDVI, GNDVI, RGVI & BNIR (Tab.1).

Table 1: Spectral indices used in the study

Index	*Name*	*Equation*	*Reference*
NDVI	*Normalised Differential Vegetation Index*	(B08 - B04) / (B08 + B04)	(Rouse et al. 1974)
GDNVI	*Green Normalised Differential Vegetation Index*	(B08 - B03) / (B08 + B03)	(Gitelson et al. 1996)
RGVI	*Red-Green-Vegetation Index*	(B03 - B04) / (B03 + B04) + 0.5	(Motohka et al. 2010), *edited*
BNIR	*Based Near Infrared*	B08 / 5500	*own equation*

The final index array contains an index value for each acquisition date, where an observation is available as well as NoData values for dates without an observation.

As a first step we eliminate outliers by removing so called “jumpy” data points from the time series. “Jumpy” data points are observations that show an unnaturally sudden ‘down-and-up-again’ pattern. In forests, re-greening processes (successive recovery) after a decrease (disturbance) occur rather slowly as compared to agricultural land, for example. Thus, such short-term dropped data points are classified as outliers and excluded from the time series.

We distinguish two main periods in the TSA process: a) the model period (MP), and b) the deviation period (DP). The model period comprises one or more full years. It is used to compute the phenology model course. The deviation period is an arbitrary period, which is examined in terms of anomalies from the phenology model course. Both periods are initially set. In this study, MP is set to 2017-2019 and DP is set to Jan. 1st, 2018 – Dec.31st, 2019.

Depending on the period (MP or DP), one must apply different TSA-tools and settings (Hirschmugl et al. 2017). At different stages of the workflow, the proposed framework combines the strengths of several TSA-approaches by using (a) curve fitting, (b) trajectory fitting and (c) trajectory segmentation.

First, a general curve fitting procedure smooths the index courses. Second, the curve fitted courses of each year within the MP are fused to one combined model course. Third, trajectory fitting as well as trajectory segmentation is applied on smoothed index courses in the DP to describe the amplitude and type of deviation from the projected model course.

In the following, the processing steps are described in detail. Before smoothing, synthetic NoData gaps are linearly interpolated to receive a continuous time series vector. Then, we apply a two-part Savitzky-Golay-Filter (SGF) (Savitzky and Golay 1964) to get two improved curves, one course for the MP data and one for the DP data. The SGF is a moving-window filtering method, calculating polynomial functions of n-degree, allowing to stay temporally sensitive. The SGF is applied using two different window settings. The first SGF uses a dynamic and wider moving window size (depending on the standard deviation of all

data points in the MP). This SGF results in stronger smoothing effects of coniferous pixels with low seasonal phenology dynamics. Here a wider SGF-window removes superfluous noise effects. Later, the resulting course is used for phenology modelling. The second SGF uses a fixed and narrower moving window (default: 31 days). The resulting index course is used for the later anomaly detection in the deviation period.

Phenology modelling and phenology metrics

The phenology modelling procedure relies on single year snippets of full years as specified by the model period. Therefore, the smoothed multi-year course is split into three parts (2017, 2018 and 2019). The multi-year-fusion is done by calculating the 10th-, 50th, and 90th-percentile of the overlaid yearly index courses. In addition, we calculate a mean of the 10th- and 90th-percentile courses to derive a so called 10th-90th-mean. We implemented an optional year weighting, which -however- was not used in this study. The year weighting could define the importance of single years for the course modelling. For example, one can continuously fade the impact of previous years or deliberately reduce the impact of years with extreme weather conditions.

The result is a 365-day course, duplicated to again cover the whole time period of the TSA (projected phenology course). The set of reconstructed percentile courses expresses the index variability within the model period and allows different perspectives for the later anomaly analysis. We defined the 10-90th-mean to be the main phenology course (MPC) for the TSA.

Finally, different forest phenology metrics can be extracted from the MPC via a percentile transition analysis (PTA), closely in line with the approach of Qiu et al. 2018. From the 5th-percentile to the 95th-percentile every 5th-percentile value is calculated. Further, we derive model transition dates for each percentile value and expressed as Day-of-Year (DOY). One model transition date is the date when the MPC first reaches the percentile value and second model transition date is when the MPC last lies above the percentile value.

The stepwise percentile transition computing (PTA) deduces several phenological metric outputs for an easier thematic interpretation of the seasonal course, e.g. start of vegetation period (SVP), end of vegetation period (EVP), length of growing biomass (LGB), number of phenology peaks and many more. For convenience only, this study shows SVP and EVP as examples for such phenology metrics.

Anomaly detection

For anomaly detection, we use the detection of index deviations from the ‘expected’ phenology course in the deviation period. The MPC can be such a ‘expected’ phenology course. However, the MPC possibly shows effects of slightly shifted courses along the time axis, e.g. due to a minimal varying start of the growing season in the DP. Furthermore, the MPC allows no value noise along the index-axis.

Therefore, an adjusted base line (BL) is required. The BL course is the “inner hull” of the MPC. In most cases this inwards buffered course serves as an adequate reference to derive meaningful dynamics of forest disturbance. It includes acceptable uncertainties index anomalies along the value as well as time axis.

Here we choose the Red-Green-Vegetation-Index (RGVI) as the index for forest disturbance mapping. Based on the MPC (10-90th percentile mean) of the RGVI, a base line (BL) is generated for the forest disturbance detection.

The cumulative sum (extensive integral) of the difference between the BL and the smoothed index course within the DP, serves as a proxy of how disturbances emerge and manifest themselves (Verbesselt et al. 2010a, b; Deijns et al. 2020). Periods with an insufficient number of data points (often winter times) are ignored for the cumulative sum calculation. Periods with a sufficient data availability are defined by the 2^{nd}- and the 98^{th}-percentile of DOY-values of all observations in the MP. In addition, the last n data points (default n=1) at the end of the time series can be truncated to avoid wrong results induced by data points that cannot be filtered and smoothed by following data points. If necessary, this step can be deactivated, e.g. when executing a rapid change detection after a storm event.

The TSA distinguishes between different forest disturbance levels (FDL). Here we sum-up daily index deviations from the BL (like an integral calculation). The increasing cumulative index deviation can reach certain values or damage levels. The so-called Cumulative Deviation Date (CDD) describes a specific date, when such a cumulative stage of deviation is reached. Different detection sensibilities can be derived by computing multiple of those forest disturbance levels. The higher the FDL, the more confirmed is the forest disturbance. This study computed 6 FDLs from 5-10, but in the following -for convenience only- we show results of a medium FDL of 7 to demonstrate the functioning of the forest disturbance detection approach.

Finally, Forest Disturbance Dates (FDDs) retrospectively reconstruct the corresponding dates of origin of disturbances depicted by the CDDs. The FDD is a “theoretical” date when the actual (non-modelled) index course last intersects with the BL. As the FDD represents the temporal origin of a forest disturbance it can possibly lies previous of the defined deviation period. The combination of CDDs and their related FDDs enables to derive information about the spatio-temporal dynamic of disturbance (e.g. duration or slope of change).

All features (CDD, FDD etc.) are exported as grids with a spatial resolution of 10 m. So as a result, you get maps that report for each Sentinel-2 pixel within the AOI if it shows any anomalies and if true an estimate for the date when the event has started as well as the magnitude of index change.

Evaluation - Plausibility check

A plausibility check compares our TSA results with change detection results derived from a selected set of date-to-date index difference layers, often used for a simple but straight-forward change detection. This evaluation helps to identify and discuss the quality of the TSA results.

We analysed a sequence of possibly cloud free imagery to validate plausibility of the forest disturbance mapping results. From three L1C-granules (Sep.8th 2017, Sep.18th 2018 & Sep.18th 2019) we used a 4x2.7km subset, with a forest area of approx. 700 hectares, to calculate RGVI values and further perform a scene-to-scene index difference between the three acquisition dates, dividing the deviation period in two annual sub-periods (2018 & 2019). The index difference layers were merged and a Δ-index-threshold of -0.075 was applied to differ changed from non-changed areas. Finally, a confusion matrix is created from the combined Δ-index outcome and the FDD result of a medium FDL-7.

Implementation

The entire workflow is implemented via the open source software 'R' (R Core Team 2019), benefitting of its comprehensive package libraries, primarily *raster* (Hijmans 2020), *rgdal* (Bivand et al. 2019), *gdalUtils* (Greenberg and Mattiuzzi 2020), *rgeos* (Bivand and Rundel 2019), *doParallel* (Microsoft Cooperation and Weston 2019), *foreach* (Microsoft Cooperation and Weston 2020) & *signal* (Signal Developers 2013). All processed data is saved on a local 'Network Attached Storage' (NAS). The approach highly relies on memory-optimised parallelising computing: first during the parallelised batch-mode of Sen2Cor, second when reading the data from our NAS to our local environment and third when executing the per-pixel TSA itself. The implemented parallelisation allows to fully use all CPU-power available.

Results

Following the structure of the method section, the results section present main findings on (1) the phenology modelling with Sentinel-2 time series of Austrian forests and (2) on the multi-year forest disturbance mapping, focusing on the extent of vast bark beetle infestation in Northern Austria (Upper- and Lower Austria) between 2018 and 2019.

Phenology Modelling with Sentinel-2 time series of Austrian forests

The phenology modelling procedure results in around 400 million unique models per spectral index, covering more than 40.000 km² of forest area in Austria, i.e. one model per pixel and per spectral index. The models cover three years of Sentinel-2 data (MP = 2017-2019). The resulting phenology courses are plotted together with detailed additional information as shown in Fig.1 and Fig. 2.

The white dots around the model courses indicate valid data points. The blue circles at the bottom of the plot show all available data points (from granules with >80% valid pixels), including observations that

were eliminated, e.g. due to clouds or shadows. The grey dots are data points excluded by the outlier filtering approach for 'jumpy' data points. The brownish ribbon illustrates the confidence interval of the MPC. Each sub-plot of the index compilation comprises the 10^{th}-percentile index course (thin red line), the 90^{th}-percentile index course (thin green line) and the resulting MPC (bold dark green line).

The pixel plots show significant differences depending on the forest type. In addition, the seasonal course patterns typical for different forest types vary from index to index. Pixels representing deciduous forest (Fig.1) show generally more variation over the year than pixels representing coniferous forest (Fig. 2).

The average NDVI- and RGVI-values are higher compared to the GNDVI- and BNIR-values, both for deciduous and coniferous forest. The seasonal course pattern of MPC is less distinct for GNDVI and RGVI than for NDVI and BNIR. The latter shows an apparent peak in spring to early summer, highlighting the BNIR's higher sensitivity to depict vegetation productivity. These temporal differences of the MPCs underline the distinct character of different spectral indices. Coniferous show little dynamic index courses. Here, the RGVI course is particularly unremarkable and continual.

Fig.1: Phenology modelling and metrics of NDVI, GDNVI, RGVI and BNIR based on data fusion of 2017-2019 for a deciduous forest pixel

The GNDVI and NDVI confidence intervals of deciduous pixels are lower than those of the BNIR and RGVI models. The RGVI noise of coniferous pixels is clearly the lowest compared to the other indices, whereas RGVI noise of deciduous forest pixels is the highest.

Fig. 2: Phenology modelling and metrics of NDVI, GDNVI, RGVI and BNIR based on data fusion of 2017-2019 for a coniferous forest pixel

The vertical lines in blue indicate three selected phenology metrics. The first one (solid line) denotes the date when MPC reaches its maximum (MPC_{Max}). Deciduous forest pixels show basically higher MAX_{MPC} values than coniferous forest pixels (Fig.1 and Fig. 2). Fig. 3 maps the MAX_{MPC} of the NDVI in Austrian forests. Values higher than 0.8, are found in areas covered by broadleaf forest, such as in the north-eastern part of Austria. NDVI values around 0.65 indicate spruce-dominated areas, as in alpine regions as well as north the Alps in Upper and Lower Austria. Lowland pine stands (e.g in Tyrol or south of Vienna) and high-alpine dwarf pines show low values about <0.55.

Fig. 3: Maximum MPC value in terms of NDVI (MAX_{MPC}) for areas covered by forest in Austria

Two dashed lines in spring and fall (Fig.1 and Fig. 2) show the start date of vegetation period (SVP) and the end date (EVP). SVP and EVP slightly differ between indices and can significantly vary between different forest types and locations (Fig. 4). Fig. 4 shows the SVP for Vorarlberg, the most western region of Austria, derived from a GNDVI model of the years 2017 to 2019. Earlier SVP mainly occur in areas dominated by broadleaf species (mainly on low to mid altitudes) and later SVP are mainly found in areas covered by coniferous forest (see slopes of the alpine south). At a closer look, one can also see

heterogeneous spatial patterns and distinct differences of the SVP at stand level that can be explained by differences in the tree species composition (Fig. 4, right).

Fig. 4: Start of vegetation period (SVP), derived from the modelled GNDVI course in the forests of the state of Vorarlberg

Forest Disturbance Mapping in Northern Austria

The forest disturbance mapping is based on the RGVI. The index proved to be the best index for negative deviation detection, as it shows little noise and robust courses on coniferous pixels (Fig. 2). Our study investigates forest disturbances in Northern Austria (Upper- and Lower Austria) by using a MP from 2017-2018 and a DP from Jan. 1st,2018 – Dez. 31st,2019. The cumulative deviation threshold is set to 7 (FDL-7) corresponding to a medium deviation level.

First, we exemplify the basic results of the anomaly detection procedure using four pixels (P1 to P4) selected from the study area (Fig. 5).

Example P1: In 2018, the first year of the deviation period (DP), the index course shows the same stable and inconspicuous trend as the year before. However, in 2019 we observe gradually lower values, some of them below the confidence interval (brownish ribbon). The red area below the blue change detection baseline (BL) indicates the cumulative deviation of the time series. In early June 2019, a strong disturbance occurs, finally reaching the deviation level CDD-7 on June 30th (orange square). February 9th 2019 can be reconstructed as the theoretical origin date of the disturbance (FDD-7, yellow triangle). The data points after the CDD-7 label confirm the detected disturbance.

Example P2: The pixel shows a disturbance occurring between July 13rd, 2018 and August 4th, 2018. The medium damage level (CDD-7) manifests in early September and its related FDD-7 is July 22nd, 2018. The winter period is ignored for the cumulative deviation sum (no red area). Here the main deviation clearly happens in the period where MP and DP intersect. The index course and the resulting deviation area (red area) in 2019 clearly confirms the detected disturbance in 2018.

Example P3: The time series of this pixel follows the modelled course and no change is detected, though the last but truncated data point possibly indicates a major deviation.

Example P4: Until November 2018, this pixel does not show any anomalies, but after the excluded winter period a severe change rapidly manifests with April 20th, 2019. The corresponding FDD-7 is traced back to the December 5th, 2018. This time series represents common winter dynamics, such as harvest or other forest management activities.

Note that every pixel time series shows grey dashed ellipsoids which represent last data points that were deliberately excluded. These data points are not yet integrated in the TSA.

Fig. 5: Forest disturbance detection 2018-2019 with medium detection sensitivity (FDL-7) – Compilation of single pixel courses, their individual deviation from the RGVI-model (2017-2018) and the identified CDD-7 and FDD-7.

Fig. 6 shows the FDD-7 map for a subset of the study area, including the previously presented pixels P1 to P4 (Fig. 5). The selected area is heavily affected by recurring bark beetle infestation (Hoch and Perny 2019). In the background, Sentinel-2 RGB-composites (10 m, Level L2A) acquired in Sep 2017, Sep 2018 and Sep 2019 are shown.

Fig. 6b highlights those pixels where FFD-7 is in 2018 (dark blue – blue – white). Fig. 6d additionally highlights those pixels where FFD-7 is in 2019 (white – yellow – orange – red – pink). The FFD map shows rectangular to round change areas, most with a 'nested minimum' of FDD. The detected areas with a late FDD occur in close proximity to areas with a previous change (lower FDD).

Fig. 6: Forest disturbance maps (FFD-7) for a subset of the study area for the deviation periods Sep. 2017 – Sep. 2018 (b), Sep. 2018 – Sep. 2019 (d) and Sep. 2017 – Sep. 2019 (f). The Sentinel-2 RGB-composites (10 m) are from Sep 2017 (a,b), Sep. 2018 (c,d) and Sep. 2019 (e,f). The phenology courses of the Pixels P1 to P4 are shown in Fig. 5 and described in the text.

The TSA-derived results were compared with the results from the combination of two index difference layers (ΔRGVI of Sep.8th 2017 – Sep.18th 2018 and Sep.18th 2018 – Sep.18th 2019) leading an overall accuracy (OA) of 91.1%, a Kappa value of 0.72 and a producer's and user's accuracy of 77.3% and 78.0%, respectively. Table 2 shows the confusion matrix table and Fig. 7 maps the confusion matrix.

Table 2: Confusion matrix with an overall accuracy of 91.1% and a Kappa value of 0.72

		Index difference layer results			
		Change	**No change**	**Classification overall**	**Producer accuracy**
TSA results	**Change**	**9301**	2631	11932	**78.0%**
	No change	2739	**45542**	48281	94.3%
	Truth overall	12040	48173	**60213**	
	User Accuracy	**77.3%**	94.5%		

Right positive and right negative are pixels where results match, indicating change and no change, respectively. False negative are pixels that are not detected by the TSA but by the difference layer approach and false positive are pixels that are detected by the TSA but not by the difference layer approach. Grey areas indicate areas excluded from the TSA, such as deciduous, grass/shrub and non-vegetated pixels.

Fig. 7: Mapped confusion matrix resulting from a comparison between the TSA-derived results and the results from a simple single-date index difference approach.

The FDD maps as shown in Fig. 6 can be spatially aggregated to Fig. 8. Fig. 8. illustrates three FDD-mapping products, computed for the whole study area: (a) the original map of the 10 m-TSA (shown as binary), (b) zonal statistics computed for hexagons of 100 hectares, and (c) zonal statistics at municipality level (Fig. 8Fig. 8). The first map shows disturbed and non-disturbed areas of the FDD-7 result with 10 m ground resolution. The second map presents the relative forest area of a regular 100ha-hexagon grid, which is affected by forest disturbances in 2018-2019. Forests on higher altitudes show generally less disturbance than forests in lowland areas. In total the disturbed forest area is 23.400 hectares or on average 2,8% of the AOI's forest area. The forest disturbance is not evenly distributed over the whole study area but concentrates on a few regions (Fig. 8). The third map shows the relatively affected forest area aggregated on the level of municipalities. One quarter of all municipalities show an affected forest area of even more than 4%, including primarily municipalities of the lower Mühlviertel, the Innviertel, the central region of Upper Austria and foremost the northern Waldviertel.

Fig. 8: Overview of change detection mapping products based on a medium detection sensitivity (FDD-7) on three spatial scales; (a) non-aggregated 10m FDD-7 grid, (b) percentage affected forest area aggregated on 100ha-hexagons and (c) aggregated on the municipality level

Discussion

Phenology Modelling with Sentinel-2 data

This study combines several established time series approaches to obtain an advanced approach, tailor-made for Sentinel-2 data and forestry applications.

Most approaches of recent TSA studies that use LANDSAT or Sentinel-2 data, apply harmonic regressions (ordinary least square models) on the generated time series to characterise seasonality of vegetation canopy (Zhu and Woodcock 2014; Jönsson et al. 2018; Shimizu et al. 2019; Deijns et al. 2020).

The periodic character of harmonic regression models, the fast computing time and the robust results are clear advantages of harmonic regressions and in the case of lower frequencies of data, they may be the only option for achieving robustness (Jönsson et al. 2018). However, they lack to describe phenology courses with a more segmented type of the seasonal phenology dynamics, as it is the case in forests of the mid-latitudes. Compared to vegetation in tropical regions with a more smoothed gradual phenology course, forest vegetation in the mid-latitudes goes through an inactive winter period, a sharp greening period in spring, followed by a little lower, stable state in summer, and a constant defoliation processes in fall.

The approach described in this article, balances such methodical shortcomings. Latest since the S2-B launch in spring 2018, improved data availability enables to compile very dense time series. The TSA uses all valid image parts from all available S2-granules with less than 80% cloud cover.

According to our experience so far, surface reflectance data produced with the ESA Sen2Cor algorithm still have considerable deficiencies. Due to these problems, quite a few images cannot be used in the TSA, although the original images (L1C) are fine. Thus, we clearly get denser time series with L1C data than with L2A data. On the downside, we must deal with some noise in the data mainly induced by atmospheric effects, which however we can handle, e.g. by efficient outlier filtering and smoothing. Other pre-processing procedures (e.g. ATCOR (GEOSYSTEMS 2020)), as alternatives to the Sen2Cor algorithm still needs to be tested. Consistent surface reflectance data would clearly be beneficial to further reduce signal noise effects. In particular, filtering out high outliers is still a problem in the applied TSA (Fig. 2, BNIR-outliers in May 2018 & 2019).

Improved geometric calibration (ground control calibration) as well as improved radiometric calibration of ESA's satellite twin have led to reduced spatial and reflectance signal noise.

The compiling of dense time series, together with the improved quality of the primary L1C data ultimately helps to counterbalance negative noise and distortion effects possibly affecting the phenology modelling. Furthermore, this allows the TSA approach to use modelling methods that can trace seasonal phenology developments with higher detail.

Generating dense, robust and consistent L1C time series allow to choose advanced fitting methods that preserve intra-seasonal variations (Jönsson et al. 2018). Therefore, our TSA is based on a dynamic Savitzy-Golay-smoothing (SGF) approach (Savitzky and Golay 1964) that uses a dynamic SGF-window-width, because a fixed window width can lead to insufficient or non-meaningful smoothing if the data is noisy (Jönsson and Eklundh 2004). Phenology metrics, such as the start and end of vegetation period, can be deduced for deciduous forest pixels quite easily due to the typical seasonal characteristics. For coniferous forest pixels, it is more challenging. Here the model's seasonal variation dependent smoothing factor (dynamic SGF-window width) proves to be an appropriate mean to deduce reasonable metrics not only for deciduous but also for coniferous forest pixels.

So far SGF was primarily used to smooth global remote sensing data with medium resolution (e.g. MODIS with 250m) and a wide moving window width for a higher degree of generalisation (Chen et al. 2004). The applied combination of filtering jumpy pixel values and a dynamic Savitzky-Golay curve fitting shows that the TSA is capable to use high resolution Sentinel-2 data for modelling forest phenology across various forest types and forestry growing regions in Austria. The phenology course modelling is suitable to derive specific phenology metrics (e.g. Fig. 4) as well as 365 'synthetic' index values (e.g. Vogelmann et al. 2017) for every day of the year (e.g. MPC), which can further be used for various downstream analyses.

The innovative multi-year percentile modelling approach traces high courses (90th-percentile) and low courses (10th-percentile) of single year time series, whereas the combined mean of both provides robust multi-year courses (MPC). The latter levels out extreme years, which further reduce distortion caused by possible outliers. In future, multi-year fusions of more than about five years will allow investigating spatiotemporal shifts of forest phenology patterns, such as slightly altering tree species compositions or changed growing periods, so the TSA will meet future demands linked with the increasing influence of long-term trends caused by climate change.

The described method sequence comprising certain filter-, interpolation-, smoothing- and multi-year fusion techniques, is rather resource-intensive in terms of computing time compared to simple regression-based modelling approaches. However, it is obvious that the benefits from the novel outputs together with the high temporal resolution compensate for the higher processing efforts. Both are key aspects when it comes, for example, to tracing various types of forest disturbance over time.

Forest Disturbance Mapping in Northern Austria

Cumulative sums of deviating courses to detect significant anomalies followed by a trajectory segmentation is widely used to detect temporal breakpoints in a time period of interest (Verbesselt et al. 2010a, b). These former approaches use a generalised harmonic model fitting for their underlying model from which deviations were computed. We use an underlying modelling that is temporally more sensitive. Here, the shown examples of pixel courses (Fig. 5) and the mapping of reconstructed forest disturbance dates (Fig. 6) demonstrate how forest monitoring can benefit from dynamic SGF-modelling applied to dense Sentinel-2 time series.

In the last decade bark beetle outbreaks in North America and Europe have impacted forested landscapes, local forestry and the provisioning of critical ecosystem services. The scale and intensity of many recent outbreaks are widely believed to be unprecedented (Morris et al. 2017). Therefore, we decided that our first change detection application investigates forest disturbance patterns in Upper- and Lower Austria. The northern parts of these two states experience steadily increasing damages caused by recurring bark beetles (Hoch and Perny 2019). Forest disturbance mapping demonstrates that vast landscapes show severe phenology anomalies (Fig. 6) and that the TSA approach proves to be a proper forest monitoring tool for large scale analyses.

The FDD maps Fig. 6 show, that most of the detected patches have a distinct spatial distribution pattern of FDDs. These patterns of growing regions are typical for the natural periodic spreading of bark beetles (Baier 2019). The detected disturbance can be interpreted as a temporal sequence of timber harvesting in a ring-like manner to counteract further bark beetle spreading. The deduced FDDs provide temporal information that is highly relevant for the pest control management of local forestry authorities. However, the results show the limited possibility to directly delineate different reason for the detected deviations. Downstream analyses as neighbourhood relations based on vectorised temporal output grids (e.g. FDD) or grid-based training of machine learning algorithms (e.g. RF or ANN), are needed. Furthermore, it can be

worthwhile to categorise different ‘shapes’ of deviating courses based on an advanced threshold-based trajectory segmentation (Moisen et al. 2016).

A quantitative validation of TSA-outcomes is generally difficult, as for many monitoring applications based on remote sensing data (Loew et al. 2017). Ground truth data that comprises temporal information on land cover changes is rare. However, evaluation results (Table 2 and Fig. 7) show that the forest disturbances identified by the TSA could be verified, independent from the type of disturbance, to a high degree.

False-negative areas (Fig. 7, yellow) are almost exclusively areas not yet detected by the TSA. Because last data points are not yet fully integrated in the TSA (Fig. 5, P3). As soon as the observed disturbance is verified by a second newly incoming data point, the TSA detects it. False-positive areas (Fig. 7, red) show a more dissolved distribution but can be rather found along the edges detected disturbance areas (right-positive). This can be explained by the higher sensitivity of the difference layer approach regarding the geometric accuracy of the underlying data. Compared to the TSA approach the difference layer approach is more prone to a possible spatial shift, as it relies on three observations only. In contrast, our dense time series is capable to level out such geometric distortion effects.

In this study MP and DP overlap, which should be avoided in the future and only was accepted because a consistent S2-data archive is only be provided since 2017. Although, Pixel-2 in Fig. 5 shows that even when MP and DP overlap, the anomaly detection approach is able to identify forest disturbances.

Although, the courses of the selected pixels shown in Fig. 5 also highlight certain limitations of the TSA approach. For example, anomalies that occur during the model period are challenging. In future we can face this problem by simply extending the model period and apply the optional year-weighting function with a strong weighting of the more recent model years. Depending on the individual requirements on the TSA, so e.g. what types of forest disturbances should be detected, it decides how to deal with possible forest disturbances in the pre-defined model period. For some applications, such as the detection of drought stress anomalies, it could be better to select the upper 90th-percentile model course instead of the mean model as the main model course of the TSA.

In this study, we investigated four spectral vegetation indices (Table 1, Fig.1 and Fig. 2). In general, some indices are more suitable to derive phenology metrics and others to detect different kinds of forest disturbances. The GNDVI is probably a good candidate for analyses on shifted spring greening due to seasonal drought stress. Here further research is needed. At least, in this study, which concentrates on the delineation of bark beetle related forest disturbances, the RGVI index proved to be a proper index to detect clear to marginal vegetation anomalies in the time series. The RGVI can be recommended for studies on bark beetle infestation.

Usually FDLs from 5 (very sensitive) to 10 (highly confirmed) are reasonable to use. We recommend the stepwise processing of a range of FDLs, because the comparison of a range of forest disturbance levels enables the end user and interpreter to assess the variability of the executed forest disturbance detection.

In this article, results for the forest disturbance level 7 (CDD-/FDD-7) are shown corresponding to a medium detection sensitivity (i.e. minor anomalies are not considered).

The computed maps reveal that large areas show high dynamic rates that are far from sustainable forestry management. If we assume optimal (i.e. equally distributed) age classes and a relatively low average rotation time of 60 years for spruce stands (Ledermann and Rössler 2019), an up to 1.7 % annual harvest rate is possible. Thus, from a forest management perspective, more than 4% (i.e. 2% per year) harvested forest area in the period 2018 to 2019, as it was found in some regions within the study area, clearly reveal unsustainable developments. At least a quarter of the investigated municipalities - for whatever reason - show such dynamics. This underlines the relevance of aggregated information, such as zonal statistics covering different scales and different *damage levels* for the forestry sector. Zonal statistics provide aggregated overviews and comprehensively inform policy makers and stakeholders about the certainty and extent of the forest disturbance detection outcomes.

Conclusion & Perspectives

In this study, we present the first forest phenology modelling and area-wide forest monitoring approach optimised for 10 m Sentinel-2 data. The method was successfully tested in Austria and is expected to be applicable also in many other regions all over the world.

Overall, the study shows that even with TOA data, instead of BOA data, robust forest phenology modelling is feasible. Even so, further tests with atmospherically corrected data (e.g. from ATCOR (GEOSYSTEMS 2020) or an improved Sen2Cor version) can be worthwhile. The TOA data can be replaced by BOA data without any effort. Besides, the TSA is extendable to additional input data. In a next step, an implementation of the Sentinel-2 20 m bands is planned.

The main benefit of the described approach, compared to Sentinel-2 approaches that exist so far, is its capability to derive meaningful phenology courses and to remain sensitive to depict intra-annual characteristics at the same time. Our TSA is more than a fixed sequence of single snapshots. It is capable to balance between temporal sensitivity and certainty, as different applications need differently adjusted TSA-settings. Besides the basic index choice, we can define various parameters as BL-offset from MPC, smoothing degree and many more.

Important outputs of the TSA are day-of-year spectral quantities (e.g. MAX_{MPC} for the NDVI) and seasonal metrics (e.g. start of vegetation period). These output features offer the opportunity to derive area-wide consistent wall-to-wall products. They are relevant to NFIs for many purposes.

Recent efforts of the Austrian NFI aim for an operational implementation to use phenology modelling metrics to derive reliable nation-wide forest types maps. Forest type classifications (Fassnacht et al. 2016) will definitely benefit from such a consistent input data. The resulting forest type maps can, for example, further improve NFI’s biomass estimations (Puliti et al. 2020).

The main added value of the presented TSA is the provision of novel temporal information about forest phenology anomalies. The TSA does not only map phenology anomalies with a high spatial resolution but also assigns a time stamp to each disturbed pixel with a high temporal resolution indicating the estimated date when the anomaly is recognizable in the dataset the first time. The high sensitivity of the TSA's outcomes serves forestry and forest ecosystem sciences aim to monitor future forests. Finally, the TSA also opens new fields for various applications on a forest management level. Here the described area-wide application, which focuses on bark beetle damages, demonstrates that the TSA-tool is a useful monitoring tool to scrutinise spatiotemporal patterns of forest disturbance. The results of this study show that it is possible to reconstruct the periodic spreading of bark beetle disturbances.

The validation of the results has been done mainly by visual inspections so far due to the lack of geo-referenced ground truth data. Additional validation with proper ground truth data is highly necessary to reliably assess the quality of the results in a quantitative way.

Next decades demand long-term analytic tools that focus on the incremental impact of climate change effects on forest ecosystems. Therefore, subsequent development steps should extend the TSA in such a way that also trans-annual anomalies can be captured.

Abbreviations

Abbreviation	*Name*
BL	Baseline to calc deviation in DP
BOA	Below-Of-Atmosphere
CDD	Cumulative deviation date
DOY	Day-of-year
DP	Deviation period
ESA	European Space Agency
EVP	End of vegetation period
FDD	Forest disturbance date
FDL	Forest disturbance level
L1C	Level-1-C (S2-TOA product level)
L2A	Level-2-A (S2-BOA product level)
NFI	National Forest Inventory
MP	Model period
MPC	Main phenology course
MAX_{MPC}	Maximum of MPC
PTA	Percentile transition analysis
S2	Sentinel-2
SGF	Savitzky-Golay-Filter
SVP	Start of vegetation period
TOA	Top-Of-Atmosphere
TSA	Time series analysis

References

Baier P (2019) Ausbreitung. In: Hoch G, Schopf A, Weizer G (eds) Der Buchdrucker. Biologie, Ökologie, Management. Bundesforschungszentrum für Wald. Austrian Research Center for Forests (BFW), Vienna, pp 57–71

Bastin J-F, Finegold Y, Garcia C, et al (2019) The global tree restoration potential. Science 365:76–79. https://doi.org/10.1126/science.aax0848

Belgiu M, Csillik O (2018) Sentinel-2 cropland mapping using pixel-based and object-based time-weighted dynamic time warping analysis. Remote Sens Environ 204:509–523. https://doi.org/10.1016/j.rse.2017.10.005

Birdsey R, Pan Y (2015) Trends in management of the world's forests and impacts on carbon stocks. For Ecol Manag 355:83–90. https://doi.org/10.1016/j.foreco.2015.04.031

Bivand R, Keitt T, Rowlingson B (2019) rgdal: Bindings for the "Geospatial" Data Abstraction Library. Version R package version 1.4-8URL https://cran.r-project.org/package=rgdal

Bivand R, Rundel C (2019) rgeos: Interface to Geometry Engine - Open Source ('GEOS'). Version R package version 0.5-2URL https://cran.r-project.org/package=rgeos

Breidenbach J, Waser LT, Debella-Gilo M, et al (2020) National mapping and estimation of forest area by dominant tree species using Sentinel-2 data. 35

Bullock EL, Woodcock CE, Olofsson P (2020) Monitoring tropical forest degradation using spectral unmixing and Landsat time series analysis. Remote Sens Environ 238:110968. https://doi.org/10.1016/j.rse.2018.11.011

Chen J, Jönsson Per, Tamura M, et al (2004) A simple method for reconstructing a high-quality NDVI time-series data set based on the Savitzky–Golay filter. Remote Sens Environ 91:332–344. https://doi.org/10.1016/j.rse.2004.03.014

Deijns AAJ, Bevington AR, van Zadelhoff F, et al (2020) Semi-automated detection of landslide timing using harmonic modelling of satellite imagery, Buckinghorse River, Canada. Int J Appl Earth Obs Geoinformation 84:101943. https://doi.org/10.1016/j.jag.2019.101943

Erb K-H, Kastner T, Plutzar C, et al (2018) Unexpectedly large impact of forest management and grazing on global vegetation biomass. Nature 553:73–76. https://doi.org/10.1038/nature25138

European Space Agency (2020a) Copernicus Programme. https://www.esa.int/Applications/Observing_the_Earth/Copernicus. Accessed 26 Apr 2020

European Space Agency (2020b) Sentinel-2 mission. https://sentinel.esa.int/web/sentinel/missions/sentinel-2. Accessed 26 Apr 2020

European Space Agency (2020c) Open Access Hub. https://scihub.copernicus.eu/twiki/do/view/SciHubWebPortal/APIHubDescription. Accessed 26 Apr 2020

European Space Agency (2020d) Sen2Cor v2.5.5

FAO Forests, the global carbon cycle and climate change. http://www.fao.org/3/XII/MS14-E.htm. Accessed 26 Apr 2020

Fassnacht FE, Latifi H, Stereńczak K, et al (2016) Review of studies on tree species classification from remotely sensed data. Remote Sens Environ 186:64–87. https://doi.org/10.1016/j.rse.2016.08.013

Gabler K, Schadauer K (2006) Methods of the Austrian Forest Inventory 2000/02. Origins, approaches, design, sampling, data models, evaluation and calculation of standard error. Austrian Research Center for Forests (BFW)

García-Mora TJ, Mas J-F, Hinkley EA (2012) Land cover mapping applications with MODIS: a literature review. Int J Digit Earth 5:63–87. https://doi.org/10.1080/17538947.2011.565080

GEOSYSTEMS (2020) ATCOR Workflow for IMAGINE. GEOSYSTEMS, Germering, Germany

Gitelson A, Kaufman Y, Merzlyak M (1996) Use of a green channel in remote sensing of global vegetation from EOS-MODIS. Remote Sens Environ 58:289–298

Goetz S, Dubayah R (2011) Advances in remote sensing technology and implications for measuring and monitoring forest carbon stocks and change. Carbon Manag 2:231–244. https://doi.org/10.4155/cmt.11.18

Greenberg JA, Mattiuzzi M (2020) gdalUtils: Wrappers for the Geospatial Data Abstraction Library (GDAL) Utilities. Version R package version 2.0.3.2URL https://cran.r-project.org/package=gdalUtils

Hansen MC, Potapov PV, Moore R, et al (2013) High-Resolution Global Maps of 21st-Century Forest Cover Change. Science 342:850–853. https://doi.org/10.1126/science.1244693

Henders S, Persson UM, Kastner T (2015) Trading forests: land-use change and carbon emissions embodied in production and exports of forest-risk commodities. Environ Res Lett 10:125012. https://doi.org/10.1088/1748-9326/10/12/125012

Hermosilla T, Wulder MA, White JC, Coops NC (2019) Prevalence of multiple forest disturbances and impact on vegetation regrowth from interannual Landsat time series (1985–2015). Remote Sens Environ 233:111403. https://doi.org/10.1016/j.rse.2019.111403

Hijmans R (2020) raster: Geographic Data Analysis and Modeling. Version R package version 3.0-12URL https://cran.r-project.org/package=raster

Hirschmugl M, Gallaun H, Dees M, et al (2017) Methods for Mapping Forest Disturbance and Degradation from Optical Earth Observation Data: a Review. Curr For Rep 3:32–45. https://doi.org/10.1007/s40725-017-0047-2

Hoch G, Perny B (2019) Die anhaltende Borkenkäfer-Kalamität in Österreich. BFW Praxisinformation 49:18–21

Jönsson P, Cai Z, Melaas E, et al (2018) A Method for Robust Estimation of Vegetation Seasonality from Landsat and Sentinel-2 Time Series Data. Remote Sens 10:635. https://doi.org/10.3390/rs10040635

Jönsson P, Eklundh L (2004) TIMESAT—a program for analyzing time-series of satellite sensor data. Comput Geosci 30:833–845. https://doi.org/10.1016/j.cageo.2004.05.006

Kanjir U, Đurić N, Veljanovski T (2018) Sentinel-2 Based Temporal Detection of Agricultural Land Use Anomalies in Support of Common Agricultural Policy Monitoring. ISPRS Int J Geo-Inf 7:405. https://doi.org/10.3390/ijgi7100405

Kindermann G, McCallum I, Fritz S, Obersteiner M (2008) A global forest growing stock, biomass and carbon map based on FAO statistics. Silva Fenn 42:387–396. https://doi.org/10.14214/sf.244

Ledermann T, Rössler G (2019) Spruce-Climate-Rotation time

Loew A, Bell W, Brocca L, et al (2017) Validation practices for satellite-based Earth observation data across communities. Rev Geophys 55:779–817. https://doi.org/10.1002/2017RG000562

Mackey B, DellaSala DA, Kormos C, et al (2015) Policy Options for the World's Primary Forests in Multilateral Environmental Agreements. Conserv Lett 8:139–147. https://doi.org/10.1111/conl.12120

Matthews E, Payne R, Rohweder M, Murray S (2000) Pilot analysis of global ecosystems: forest ecosystems. Pilot Anal Glob Ecosyst For Ecosyst

McDowell NG, Coops NC, Beck PSA, et al (2015) Global satellite monitoring of climate-induced vegetation disturbances. Trends Plant Sci 20:114–123. https://doi.org/10.1016/j.tplants.2014.10.008

Microsoft Cooperation, Weston S (2019) doParallel: Foreach Parallel Adaptor for the "parallel" Package. Version R package version 1.0.15URL https://cran.r-project.org/package=doParallel

Microsoft Cooperation, Weston S (2020) foreach: Provides Foreach Looping Construct. Version R package version 1.4.8URL https://cran.r-project.org/package=foreach

Moisen GG, Meyer MC, Schroeder TA, et al (2016) Shape selection in Landsat time series: a tool for monitoring forest dynamics. Glob Change Biol 22:3518–3528. https://doi.org/10.1111/gcb.13358

Morris JL, Cottrell S, Fettig CJ, et al (2017) Managing bark beetle impacts on ecosystems and society: priority questions to motivate future research. J Appl Ecol 54:750–760. https://doi.org/10.1111/1365-2664.12782

Motohka T, Nasahara KN, Oguma H, Tsuchida S (2010) Applicability of Green-Red Vegetation Index for Remote Sensing of Vegetation Phenology. Remote Sens 2:2369–2387.

https://doi.org/10.3390/rs2102369

Nguyen TH, Jones SD, Soto-Berelov M, et al (2018) A spatial and temporal analysis of forest dynamics using Landsat time-series. Remote Sens Environ 217:461–475. https://doi.org/10.1016/j.rse.2018.08.028

O'Hara KL (2016) What is close-to-nature silviculture in a changing world? For Int J For Res 89:1–6. https://doi.org/10.1093/forestry/cpv043

Pasquarella V, Bradley B, Woodcock C (2017) Near-Real-Time Monitoring of Insect Defoliation Using Landsat Time Series. Forests 8:275. https://doi.org/10.3390/f8080275

Pugh TAM, Lindeskog M, Smith B, et al (2019) Role of forest regrowth in global carbon sink dynamics. Proc Natl Acad Sci 116:4382–4387. https://doi.org/10.1073/pnas.1810512116

Puliti S, Hauglin M, Breidenbach J, et al (2020) Modelling above-ground biomass stock over Norway using national forest inventory data with ArcticDEM and Sentinel-2 data. Remote Sens Environ 236:111501. https://doi.org/10.1016/j.rse.2019.111501

Qiu B, Zou F, Chen C, et al (2018) Automatic mapping afforestation, cropland reclamation and variations in cropping intensity in central east China during 2001–2016. Ecol Indic 91:490–502. https://doi.org/10.1016/j.ecolind.2018.04.010

R Core Team (2019) R: A language and environment for statistical computing. R Foundation for Statistical Computing. Vienna, Austria

Rouse JW, Haas RH, Scheel JA, Deering DW (1974) Monitoring Vegetation Systems in the Great Plains with ERTS. In: Proceedings, 3rd Earth Resource Technology Satellite (ERTS) Symposium. pp 48–62

Savitzky Abraham, Golay MJE (1964) Smoothing and Differentiation of Data by Simplified Least Squares Procedures. Anal Chem 36:1627–1639. https://doi.org/10.1021/ac60214a047

Sebald J, Senf C, Heiser M, et al (2019) The effects of forest cover and disturbance on torrential hazards: large-scale evidence from the Eastern Alps. Environ Res Lett 14:114032. https://doi.org/10.1088/1748-9326/ab4937

Seidl R, Albrich K, Erb K, et al (2019) What drives the future supply of regulating ecosystem services in a mountain forest landscape? For Ecol Manag 445:37–47. https://doi.org/10.1016/j.foreco.2019.03.047

Shimizu K, Ota T, Mizoue N (2019) Detecting Forest Changes Using Dense Landsat 8 and Sentinel-1 Time Series Data in Tropical Seasonal Forests. Remote Sens 11:1899. https://doi.org/10.3390/rs11161899

Signal Developers (2013) signal: Signal processing

Verbesselt J, Hyndman R, Newnham G, Culvenor D (2010a) Detecting trend and seasonal changes in satellite image time series. Remote Sens Environ 114:106–115.

https://doi.org/10.1016/j.rse.2009.08.014

Verbesselt J, Hyndman R, Zeileis A, Culvenor D (2010b) Phenological change detection while accounting for abrupt and gradual trends in satellite image time series. Remote Sens Environ 114:2970–2980. https://doi.org/10.1016/j.rse.2010.08.003

Vogelmann J, Khoa P, Lan D, et al (2017) Assessment of Forest Degradation in Vietnam Using Landsat Time Series Data. Forests 8:238. https://doi.org/10.3390/f8070238

Vrieling A, Meroni M, Darvishzadeh R, et al (2018) Vegetation phenology from Sentinel-2 and field cameras for a Dutch barrier island. Remote Sens Environ 215:517–529. https://doi.org/10.1016/j.rse.2018.03.014

Wulder MA, Loveland TR, Roy DP, et al (2019) Current status of Landsat program, science, and applications. Remote Sens Environ 225:127–147. https://doi.org/10.1016/j.rse.2019.02.015

Xue J, Su B (2017) Significant Remote Sensing Vegetation Indices: A Review of Developments and Applications. J Sens 2017:1353691. https://doi.org/10.1155/2017/1353691

Zhu Z, Woodcock CE (2014) Continuous change detection and classification of land cover using all available Landsat data. Remote Sens Environ 144:152–171. https://doi.org/10.1016/j.rse.2014.01.011

Declarations

Ethics approval and consent to participate

Not applicable

Consent for publication

Not applicable

Availability of data and materials

The datasets used and/or analyzed during the current study are available from the corresponding author on reasonable request.

Competing interests

Not applicable

Funding

Not applicable

Authors' contributions

ML prepared the imagery data, developed and implemented the time series algorithm and performed downstream analyses from the time series outputs. TK was a major contributor in interpreting the results and in writing the manuscript. Both authors read and approved the final manuscript.

Acknowledgments

Not applicable

Figures

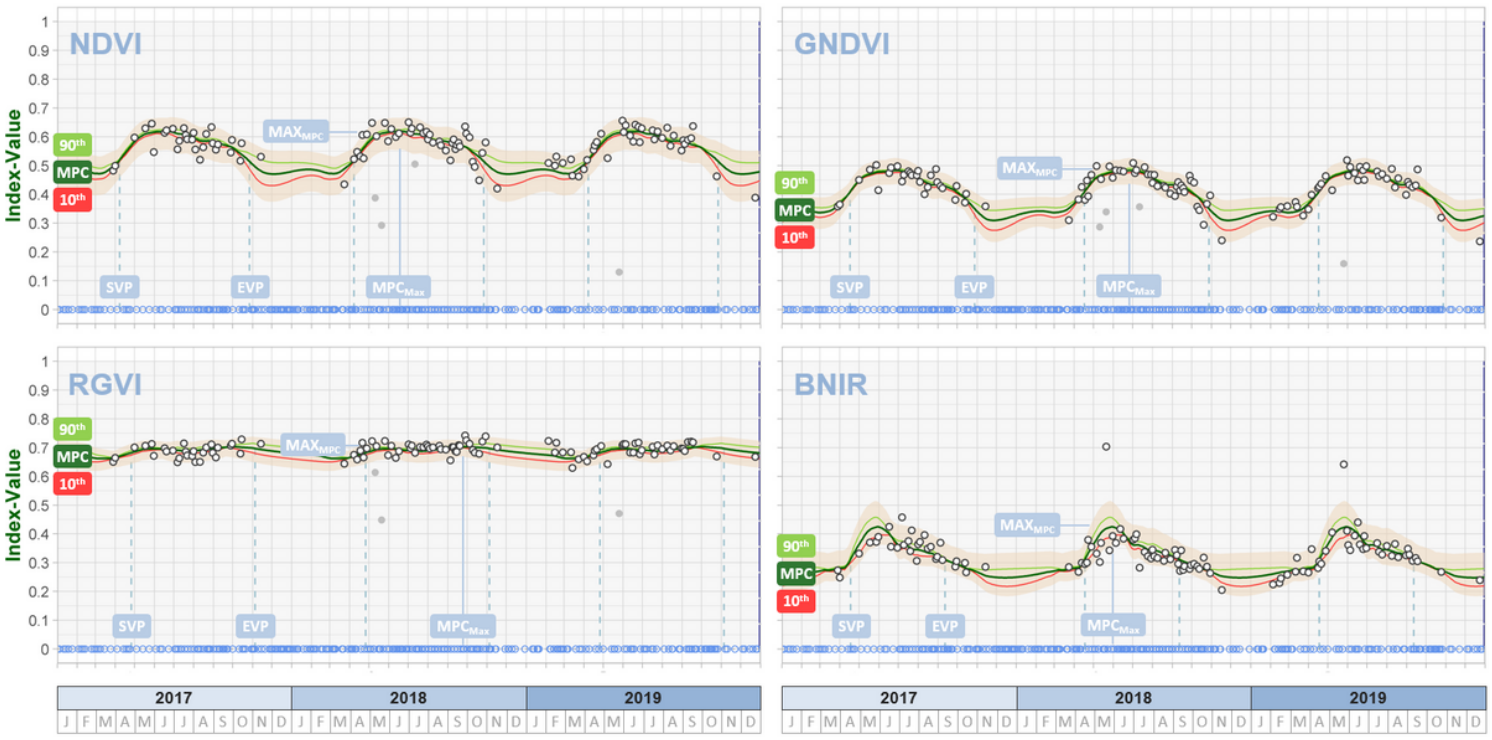

Figure 1

Phenology modelling and metrics of NDVI, GDNVI, RGVI and BNIR based on data fusion of 2017-2019 for a deciduous forest pixel

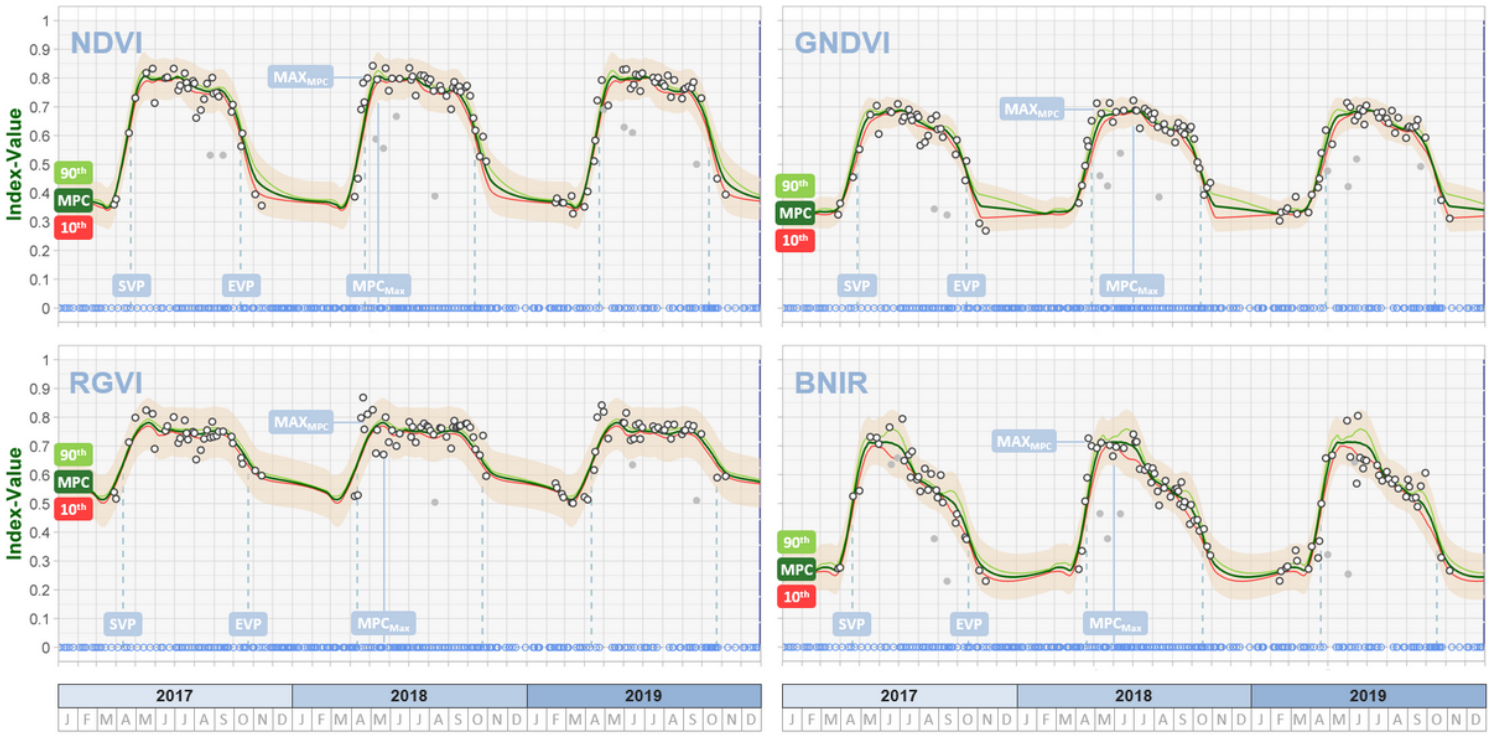

Figure 2

Phenology modelling and metrics of NDVI, GDNVI, RGVI and BNIR based on data fusion of 2017-2019 for a coniferous forest pixel

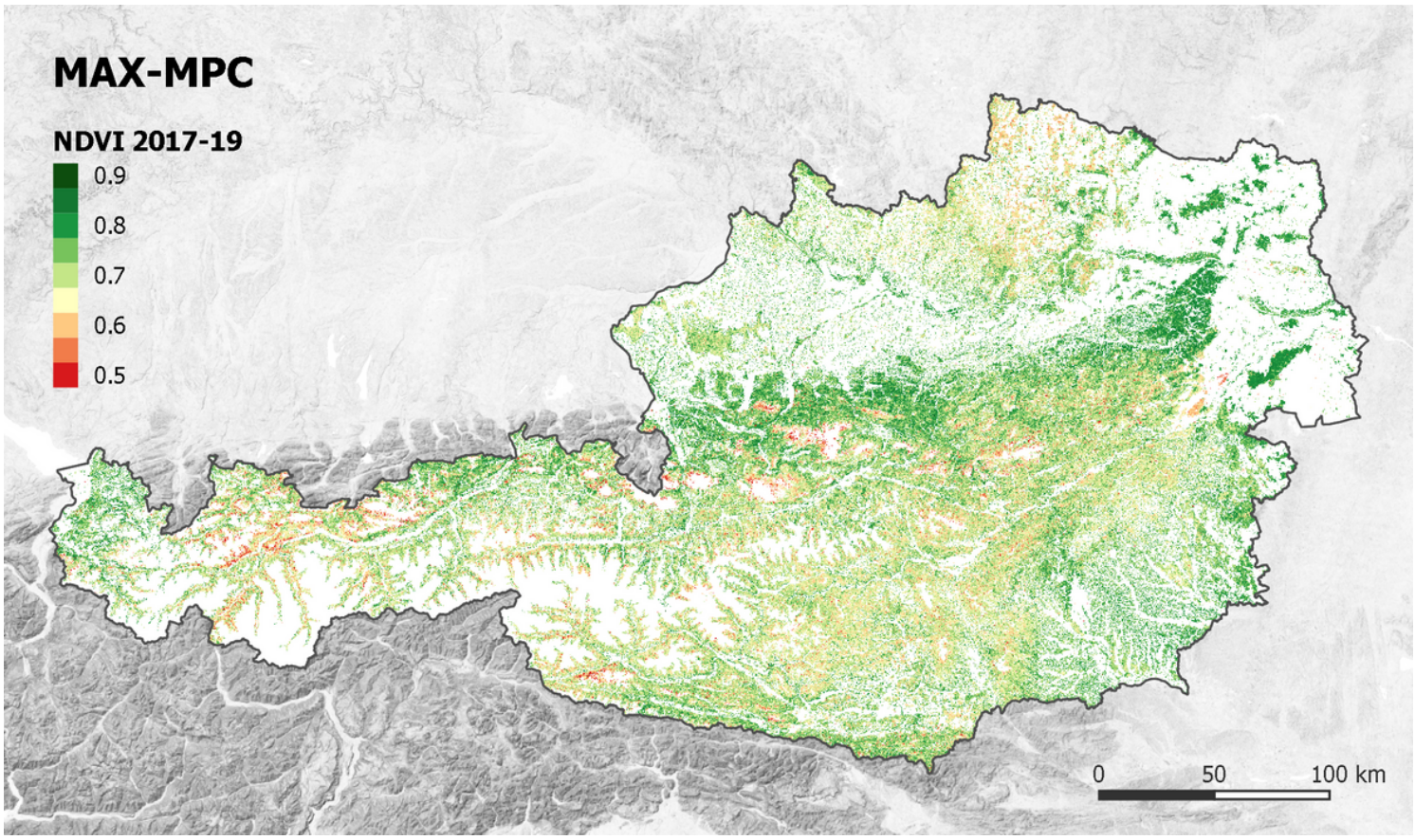

Figure 3

Maximum MPC value in terms of NDVI (MAXMPC) for areas covered by forest in Austria

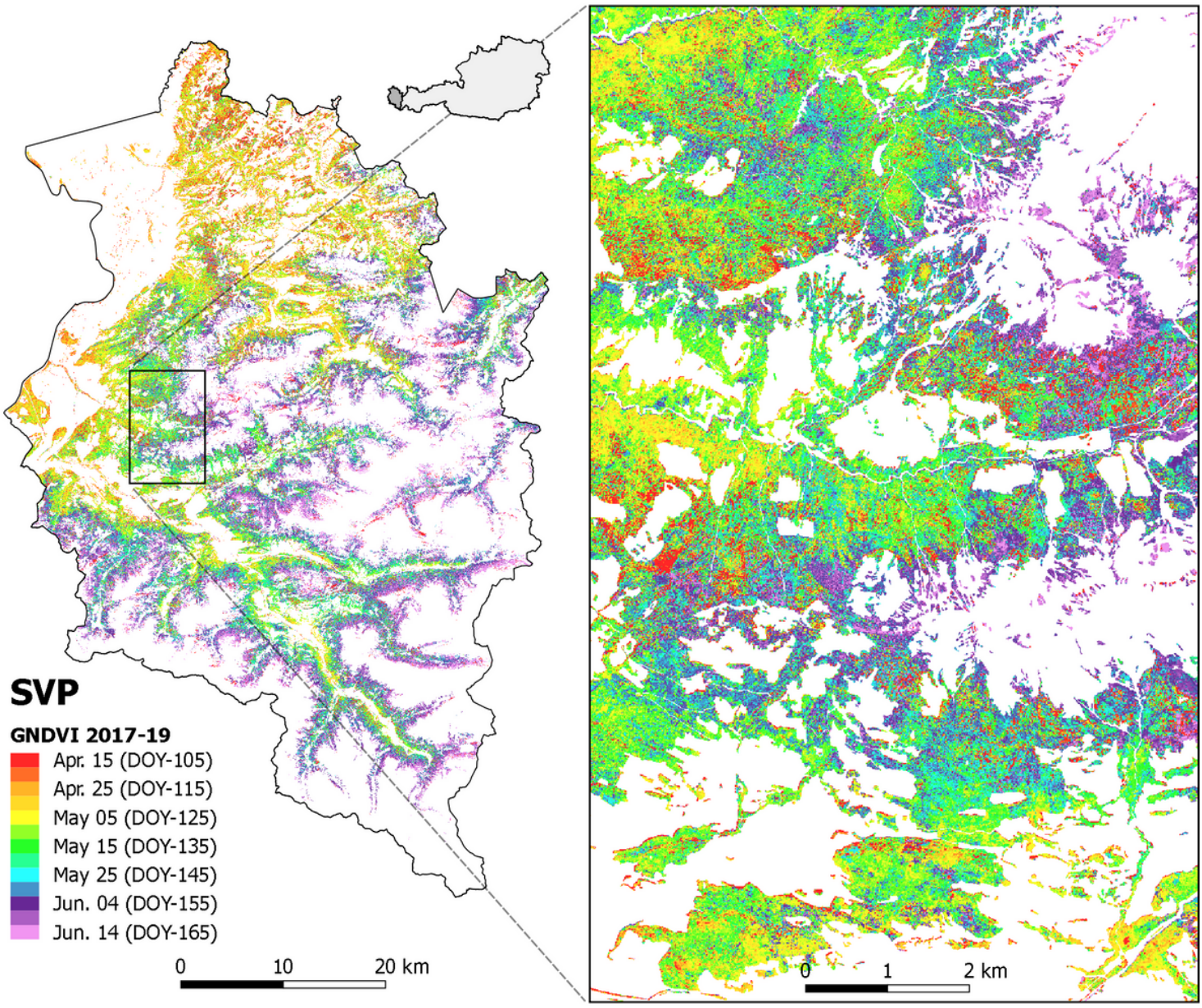

Figure 4

Start of vegetation period (SVP), derived from the modelled GNDVI course in the forests of the state of Vorarlberg

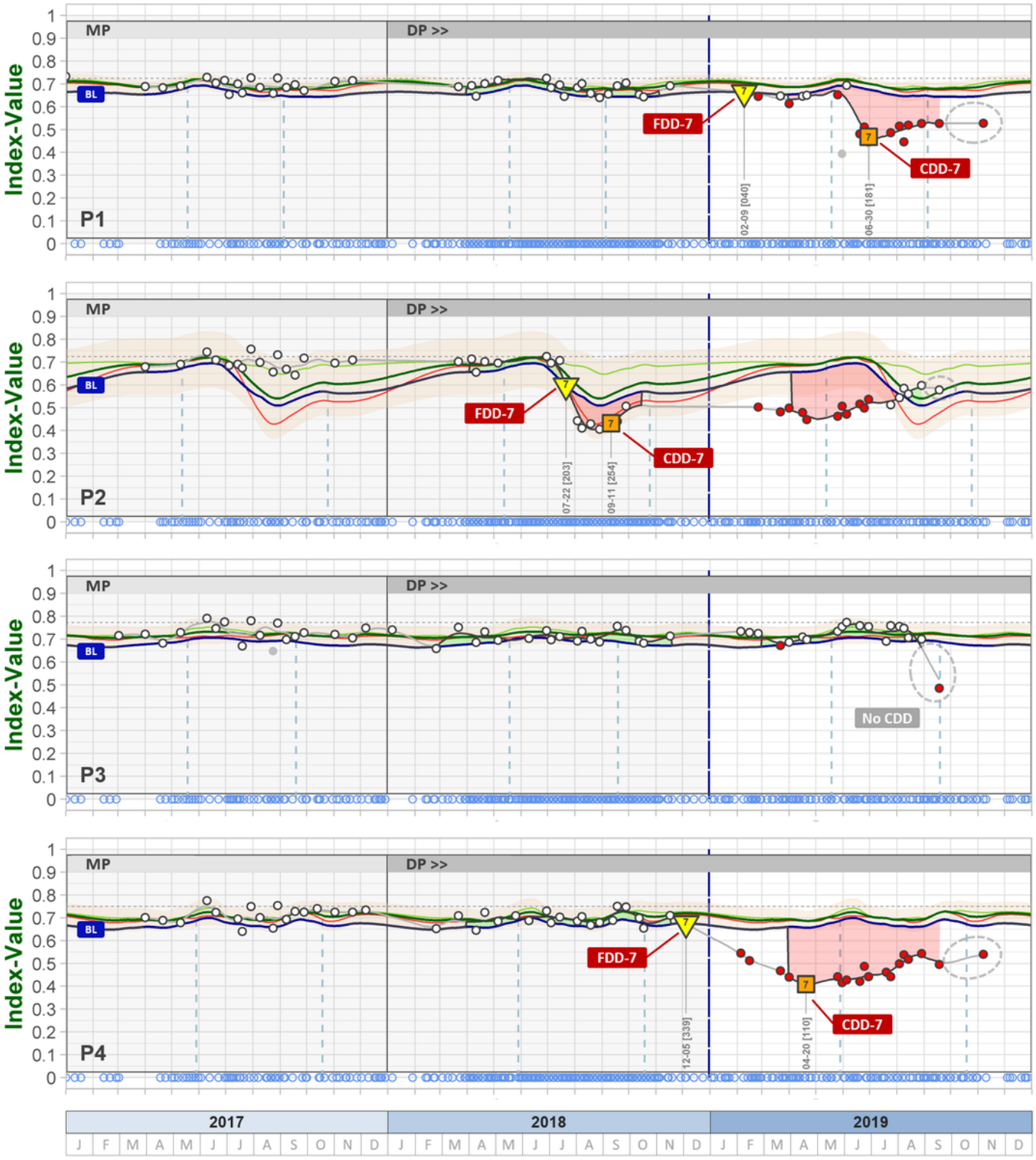

Figure 5

Forest disturbance detection 2018-2019 with medium detection sensitivity (FDL-7) – Compilation of single pixel courses, their individual deviation from the RGVI-model (2017-2018) and the identified CDD-7 and FDD-7.

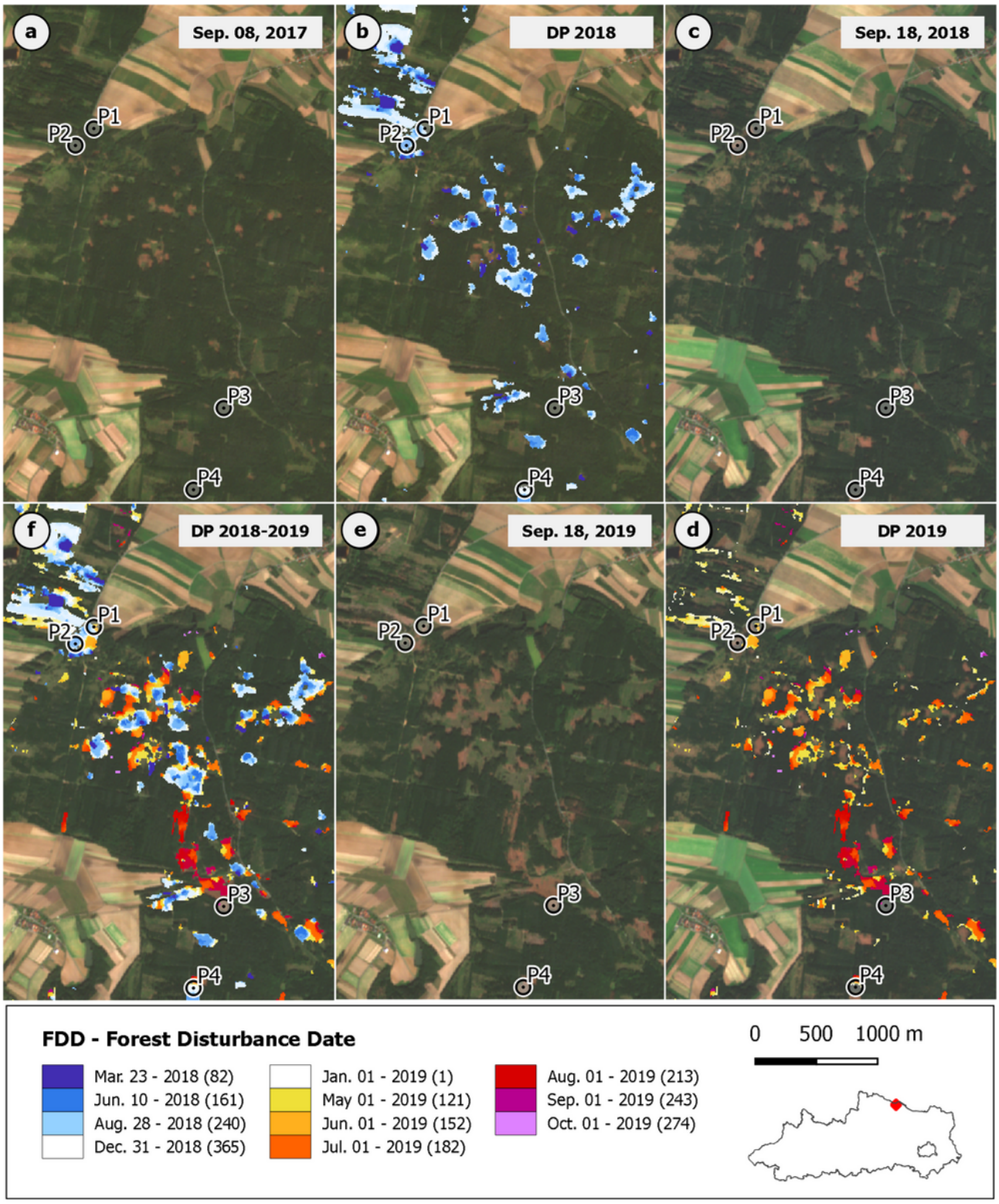

Figure 6

Forest disturbance maps (FFD-7) for a subset of the study area for the deviation periods Sep. 2017 – Sep. 2018 (b), Sep. 2018 – Sep. 2019 (d) and Sep. 2017 – Sep. 2019 (f). The Sentinel-2 RGB-composites (10 m) are from Sep 2017 (a,b), Sep. 2018 (c,d) and Sep. 2019 (e,f). The phenology courses of the Pixels P1 to P4 are shown in Fig. 5 and described in the text.

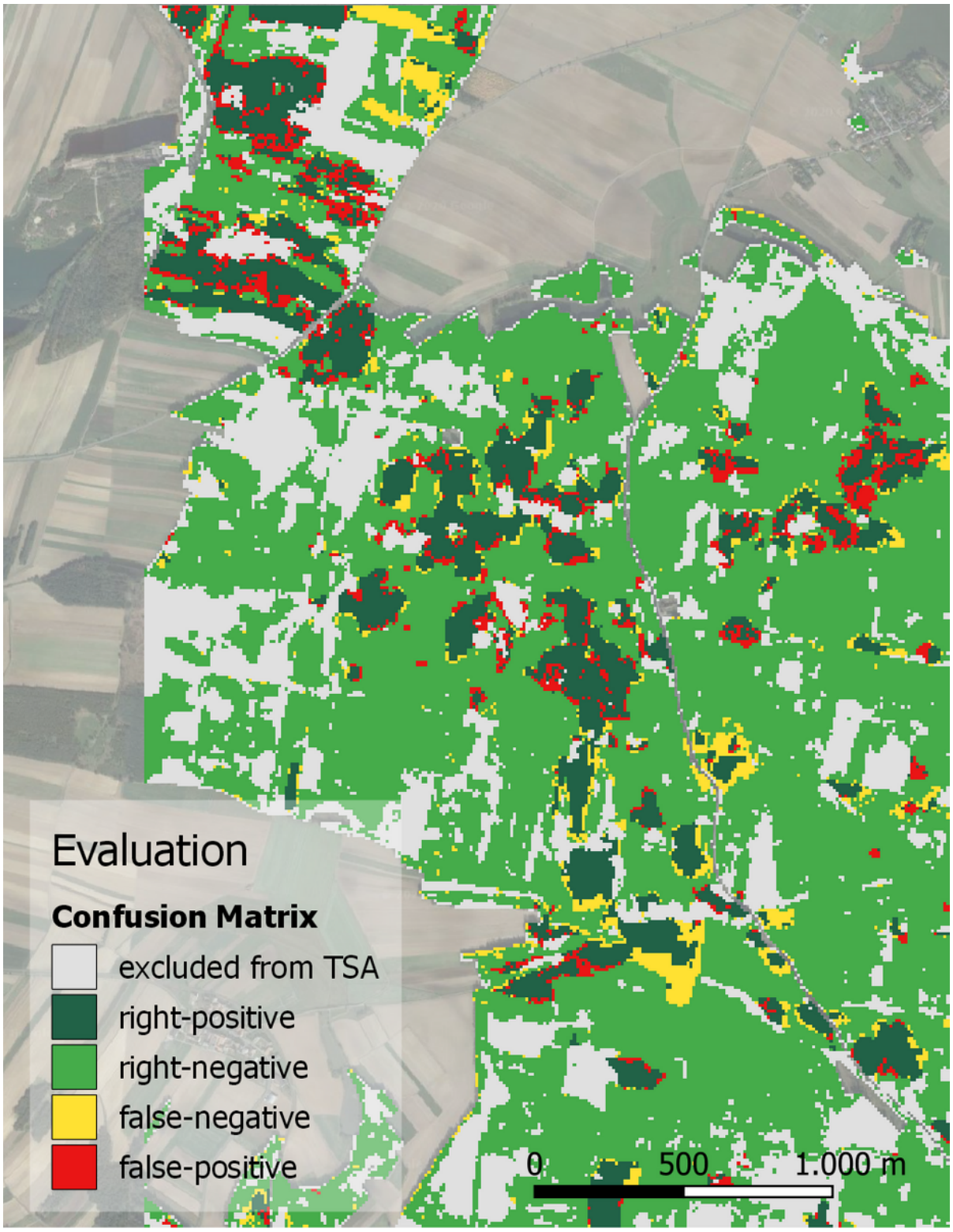

Figure 7

Mapped confusion matrix resulting from a comparison between the TSA-derived results and the results from a simple single-date index difference approach.

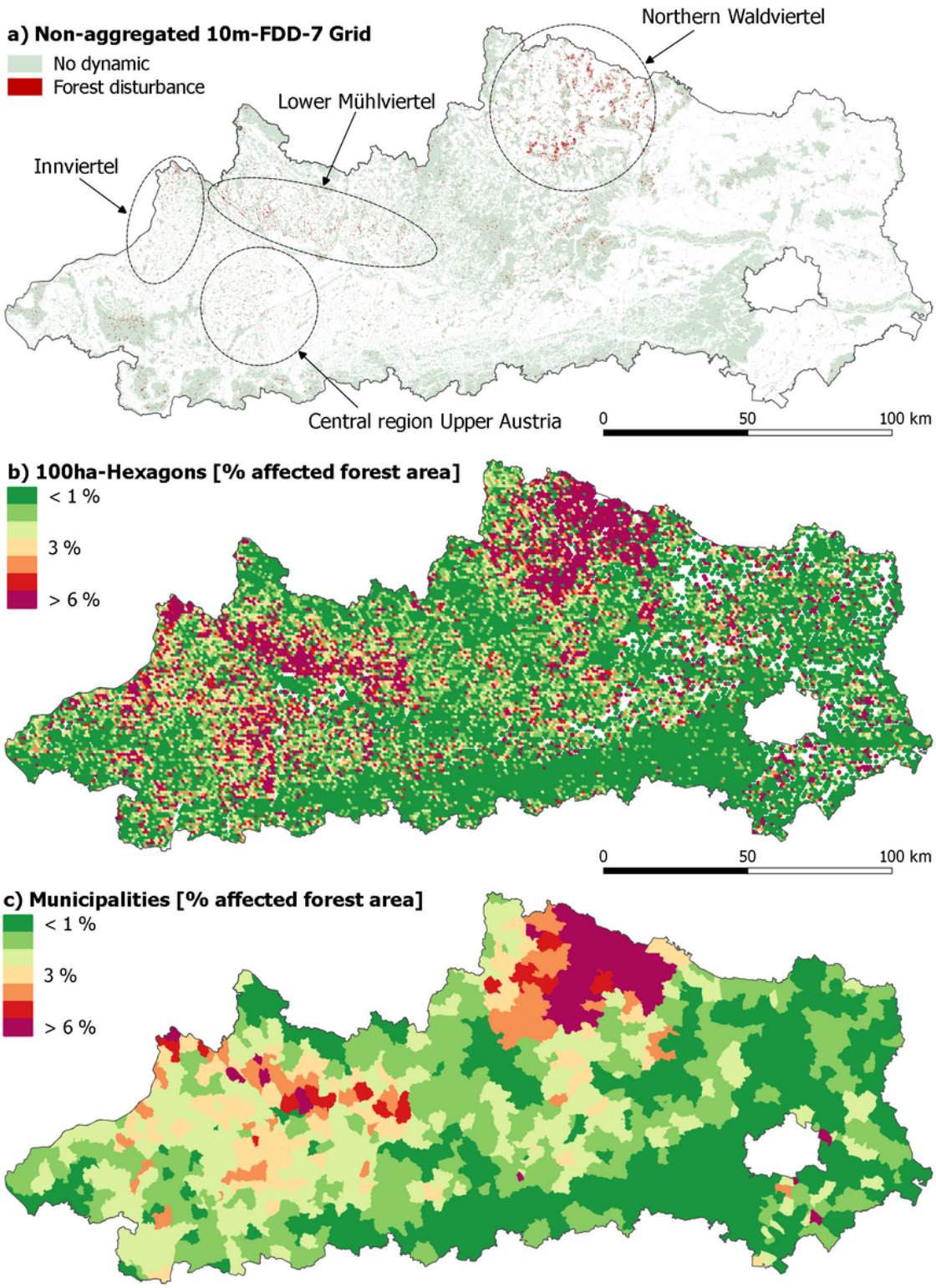

Figure 8

Overview of change detection mapping products based on a medium detection sensitivity (FDD-7) on three spatial scales; (a) non-aggregated 10m FDD-7 grid, (b) percentage affected forest area aggregated on 100ha-hexagons and (c) aggregated on the municipality level